EPJ Web of Conferences **49**, 13001 (2013)
DOI: 10.1051/epjconf/20134913001

Rare B decays and CP-Violation in the B system with the ATLAS Detector

Patrick Jussel[1,2,a]

[1] *on behalf of the ATLAS Collaboration*
[2] *University of Innsbruck, Austria*

Abstract. A search for the rare decay $B_s^0 \to \mu^+\mu^-$ has been performed with the ATLAS detector at the Large Hadron Collider LHC in proton-proton collisions at a centre of mass energy of $\sqrt{s} = 7\,\text{TeV}$ using $2.4\,\text{fb}^{-1}$ of integrated luminosity. The observed number of signal events is consistent with the background expectations and the resulting upper limit on the branching fraction is set to $\mathcal{B}(B_s^0 \to \mu^+\mu^-) < 2.2\,(1.9) \times 10^{-8}$ at 95% (90%) confidence level. A time dependent measurement of CP-violation in the exclusive decay channel $B_s^0 \to J/\psi(\mu^+\mu^-)\phi(K^+K^-)$ has been performed with an integrated luminosity of $4.9\,\text{fb}^{-1}$ at an energy of $\sqrt{s} = 7\,\text{TeV}$. The resulting measurements of the CP-violation weak mixing phase $\phi_s = 0.22 \pm 0.41\,(\text{stat.}) \pm 0.10\,(\text{syst.})\,\text{rad}$ and the decay width difference $\Delta\Gamma_s = 0.053 \pm 0.021\,(\text{stat.}) \pm 0.008\,(\text{syst.})\,\text{ps}^{-1}$ are consistent with the theoretical predictions of the Standard Model and the world average values.

1 Introduction

Heavy flavour physics in the b-quark sector is sensitive to phenomena beyond the Standard Model (SM). Mediated by flavour changing neutral currents (FCNC), the rare decay channel $B_s^0 \to \mu^+\mu^-$ is CKM suppressed, helicity suppressed and can only occur in SM via higher order electroweak Feynman diagrams. The theoretical prediction of its branching fraction is $\mathcal{B}(B_s^0 \to \mu^+\mu^-) = (3.5 \pm 0.2) \times 10^{-9}$ [1]. Models beyond the SM can increase this branching ratio, thus any deviation from the SM predictions would indicate new physics. A first evidence of this decay has been seen by the LHCb collaboration with a branching ratio of $\mathcal{B}(B_s^0 \to \mu^+\mu^-) = 3.2^{+1.4}_{-1.2}\,(\text{stat.})^{+0.5}_{-0.3}\,(\text{syst.}) \times 10^{-9}$ which is in agreement with the SM predictions.

In the exclusive decay $B_s^0 \to J/\psi(\mu^+\mu^-)\phi(K^+K^-)$ the CP-violation due to a weak phase between the $B_s^0 - \bar{B_s^0}$ mixing amplitude and the $b \to c\bar{c}s$ decay amplitude is described by the CP-violation weak mixing phase $\phi_s \simeq -2\beta_s$, where $\beta_s = \arg[-(V_{ts}V_{tb}^*)/(V_{cs}V_{cb}^*)]$ is the angle in one of the unitary triangles. The SM predicts a small value of $\phi_s = -0.0368 \pm 0.0018\,\text{rad}$ [2]. Non-SM contributions in the $B_s^0 - \bar{B_s^0}$ mixing box diagram could alter this phase, which can be parametrised by $\phi_s = \phi_s^{SM} + \phi_s^{\Delta}$, where ϕ_s^{SM} is the value predicted by SM and ϕ_s^{Δ} describes additional phase contributions due to physics beyond the SM [3]. The decay width difference $\Delta\Gamma_s = \Gamma_L - \Gamma_H$ of the B_s^0 mass eigenstates B_H (heavy) and B_L (light) is also involved in B_s^0 mixing. However, the effects of physics beyond the SM on $\Delta\Gamma_s$ are expected to be not significant [3].

This report describes the measurement of the rare decay $B_s^0 \to \mu^+\mu^-$ [4] and the untagged angular analysis of $B_s^0 \to J/\psi(\mu^+\mu^-)\phi(K^+K^-)$ decays for the measurement of ϕ_s and $\Delta\Gamma_s$ [5] by the ATLAS experiment at the LHC. Both measurements use data collected by the ATLAS experiment in pp collisions at a centre of mass energy of $\sqrt{s} = 7\,\text{TeV}$, corresponding to an integrated luminosity of $\sim 2.4\,\text{fb}^{-1}$ ($B_s^0 \to \mu^+\mu^-$) and $\sim 4.9\,\text{fb}^{-1}$ ($B_s^0 \to J/\psi\phi$). In section 2 the event selection is outlined. In chapter 3 the analysis of the decay $B_s^0 \to \mu^+\mu^-$ and its results are given, following [4]. In Section 4 the measurement of ϕ_s and $\Delta\Gamma_s$ is shown, corresponding to [5]. A summary and an outlook is given in section 5.

2 Candidate Selection

The ATLAS detector is a LHC multipurpose particle detector described in detail in [6]. For the measurements in this report the inner tracking detector and the muon system are the most important components. The inner detector consists of a pixel detector, a silicon microstrip detector and a transition radiation tracker embedded in an axial magnetic field of 2 T. The muon detector consists of tracking chambers and trigger detectors embedded in three superconducting toroidal magnetic fields. Since tracks in the inner detector are matched with tracks in the muon system, data is only used if both systems have been correctly working.

The trigger strategy for both analysis is based on a di-muon trigger to select $B_s^0 \to \mu^+\mu^-$ candidates directly or to identify $J/\psi \to \mu^+\mu^-$ decays. In both cases the di-muon trigger has a transverse momentum threshold of $p_T > 4\,\text{GeV}$ for both muon candidates.

In the $B_s^0 \to \mu^+\mu^-$ analysis the two muon candidates are fitted to a common vertex. The events are loosely se-

[a] e-mail: p.jussel@gmail.com

lected by applying a cut on 4 GeV $< m_{\mu^+\mu^-} <$ 8.5 GeV to be compatible with a B_s^0 candidate.

In the CP-violation analyses a further trigger is used in an asymmetric configuration, selecting events with a higher p_T threshold (4 GeV−10 GeV) for one of the muons and looser requirement (threshold below 4 GeV) for the second muon. The invariant di-muon mass is required to be compatible with the J/ψ mass. The ϕ candidates are obtained by combining opposing charged tracks assuming a $\phi \to K^+K^-$ decay, where the charged tracks are not identified as muons. The two muon candidates and the two kaon candidates are fitted into a common vertex with χ^2/d.o.f. < 3 to build the B_s^0 candidate, where the invariant mass of the two muons is fixed to the J/ψ mass [10]. More details on the reconstruction of $B_s^0 \to J/\psi\phi$ decay can be found in [4].

3 Measurement of the Branching Ratio of the Rare Decay $B_s^0 \to \mu^+\mu^-$

3.1 Analysis Strategy

The branching fraction $\mathcal{B}(B_s^0 \to \mu^+\mu^-)$ is measured with respect to the abundant decay $B^\pm \to J/\psi(\mu^+\mu^-)K^\pm$ in order to be independent of uncertainties of the luminosity and the $b\bar{b}$ production cross section:

$$\mathcal{B}(B_s^0 \to \mu^+\mu^-) = \frac{N_{\mu^+\mu^-}}{N_{J/\psi K^\pm}} \times \frac{\varepsilon_{J/\psi K^\pm}}{\varepsilon_{\mu^+\mu^-}} \times \frac{A_{J/\psi K^\pm}}{A_{\mu^+\mu^-}} \times \frac{f_u}{f_s} \times \mathcal{B}(B^\pm \to J/\psi K^\pm) \cdot \mathcal{B}(J/\psi \to \mu^+\mu^-),$$

where for each decay mode i the number of observed events is N_i and the absolute efficiencies and acceptances are denoted as ε_i and A_i. For both decay channels the efficiencies and acceptances are determined from Monte Carlo. The ratio of the b-quark fragmentations f_u/f_s and the branching ratios for the reference channel are taken from measurements [10, 11]. The branching ratio corresponding to one single measured event ($N_{\mu^+\mu^-} = 1$) is defined as the single event sensitivity (SES).

In order to perform a blind analysis, the signal region defined in the range (5066, 5666) MeV around the B_s^0 mass is excluded in the optimisation procedure. The data in the sidebands is split into two halves: one half for the signal/background optimisation and the other half for the measurement of the background in the search window. For the signal/background discrimination, a boosted decision tree (BDT) is trained on on half of the sideband data as background model and on reweighted signal Monte Carlo events, where for the reweighting half of the $B^\pm \to J/\psi K^\pm$ events are used. A total of 14 variables with high discriminating power are chosen for the multivariate analysis, where all variables show no correlation with the di-muon mass and are not strongly correlated to each other. The variables with the highest discrimination power are the pointing angle of the B_s^0 momentum vector, the transverse decay length and the isolation of the decay particles.

The mass resolution and thus the signal/background separation of the ATLAS detector depends on the pseudorapidity η of the muon tracks. Therefore the data is split into three invariant mass-resolution zones defined by the muon with larger pseudorapidity, $|\eta|_{max}$ in ranges of: $0-1$, $1-1.5$ and $1.5-2.5$ with approximated mass resolutions of 60, 80 and 110 MeV, respectively. For each mass-resolution category i the size of the search window Δm^i and the cut on the BDT classifier q^i_{cut} is optimised individually.

The background consists of continuous background with a smooth dependence on the di-muon mass and resonant background components. The continuous back-

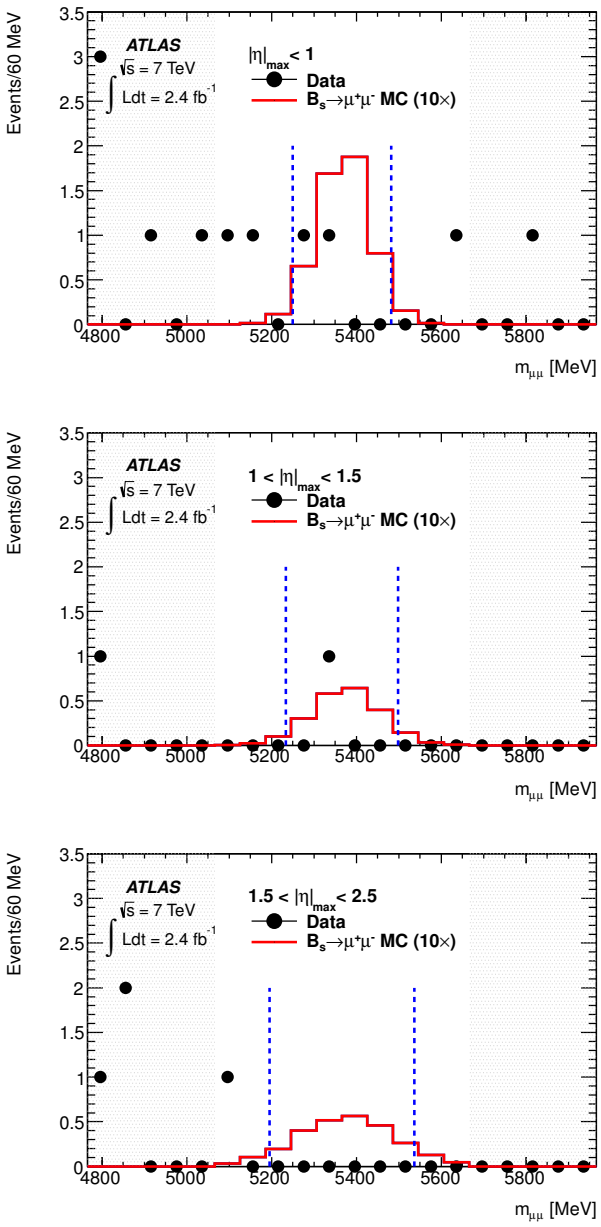

Figure 1: For each mass-resolution category i the invariant di-muon mass distribution of selected $B_s^0 \to \mu^+\mu^-$ candidates with $q > q^i_{cut}$ is shown as dots, where the horizontal dashed lines illustrate the search windows with size Δm^i and the shaded area correspond to the sidebands. The expected signal as predicted by Monte Carlo assuming $\mathcal{B}(B_s^0 \to \mu^+\mu^-) = 3.5 \times 10^{-8}$ is shown as continuous line. Figure taken from [4].

ground originates from random combination of muon tracks from various prompt (e.g. Drell-Yan) or non-prompt (mainly $b\bar{b} \rightarrow \mu^+\mu^- X$) processes. The non-resonant background in the signal region is measured by interpolation from half of the sideband data into the search region, resulting in a background scale factor R^i_{bkg} for each mass-resolution category. The uncertainty in the background scaling is common for all bins as a global factor R_{glob}. The resonant background comes from B decays, in which one or two charged tracks have been misidentified as muons due to decays in flight or punch-through of hadrons into the muon system. Since $B \rightarrow hh'$ decays cannot be distinguished from signal decays in the measurement and consequently are hard to suppress, the resonant background contribution is estimated from dedicated Monte Carlo samples. The expected number of resonant background events is shown in Table 1 for the three different resolution zones as well as the number of background counts in the sidebands and the background scale factors.

The $B^\pm$ yield is measured by a binned maximum likelihood fit of the $B^\pm \rightarrow J/\psi(\mu^+\mu^-)K^\pm$ invariant mass spectrum. For the limit extraction, the CLs method [7, 8] with a profile likelihood ratio is used. Statistical and systematic uncertainties in $\epsilon = (f_s/f_u)\mathcal{B}(B^\pm \rightarrow J/\psi(\mu^+\mu^-)K^\pm)$, $\epsilon_i = \mathcal{B}(B^0_s \rightarrow \mu^+\mu^-) = N_{J/\psi K^\pm}(A_{\mu^+\mu^-}\varepsilon_{\mu^+\mu^-})/(A_{J/\psi K^\pm}\varepsilon_{J/\psi K^\pm})$ and R_{glob} are taken into account in the limit extraction, as shown in Table 1.

3.2 Results

In Table 1 all quantities for the extraction of a limit on the branching ratio are summarised. The unblinded dimuon invariant mass distribution using the full statistics in the search window is shown in Figure 1. Using the CLs method an upper limit on the branching fraction $\mathcal{B}(B^0_s \rightarrow \mu^+\mu^-) < 2.2(1.9) \times 10^{-8}$ at 95 % (90 %) CL has been set, as shown in Figure 2. This result has been used for the first LHC-wide combination of measurements by ATLAS, CMS and LHCb on $\mathcal{B}(B^0_s \rightarrow \mu^+\mu^-)$ [9].

Table 1: Single event sensitivity SES = $(\epsilon\epsilon_i)^{-1}$ and their components, where ϵ is common to all bins and ϵ_i for each bin. Global background scaling factor R_{glob} and relative scaling factors per bin R^i_{bkg}, background counts in the sidebands N^i_{bkg}, resonant background estimates in the search region $N^i_{B\rightarrow hh'}$ and event count in the search window N^i_{obs} for the three different mass resolution categories. Table adapted from [4].

$\lvert\eta\rvert_{max}$ range	0 - 1.0	1.0 - 1.5	1.5 - 2.5.
SES (10^{-8})	0.71	1.6	1,4
$\epsilon\,(10^3)$		4.45 ± 0.45	
$\epsilon_i\,(10^4)$	3.14 ± 0.17	1.40 ± 0.15	1.58 ± 0.26
R_{glob}		1.00 ± 0.04	
R^i_{bkg}	1.29	1.14	0.88
N^i_{bkg}	5	0	2
$N^i_{B\rightarrow hh'}$	0.10	0.06	0.08
N^i_{obs}	2	1	0

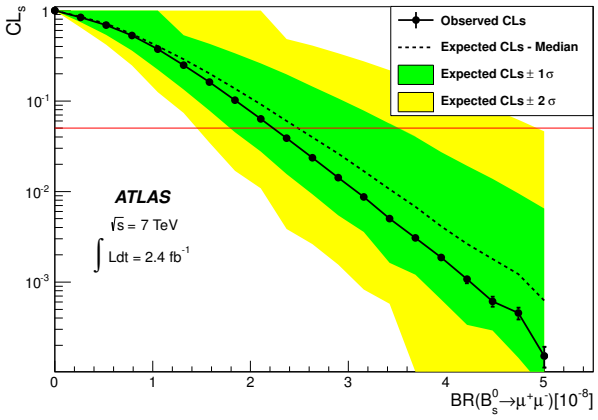

Figure 2: The observed CLs (circles) as a function of the branching fraction $\mathcal{B}(B^0_s \rightarrow \mu^+\mu^-)$. The 95 % CL upper limit corresponds to the intersection of the horizontal line with the observed CLs line. The green and yellow bands correspond to $\pm 1\sigma$ and $\pm 2\sigma$ fluctuations of the expected limit from the median of the expectation (dashed line). Figure taken from [4].

4 Measurement of the CP-violating weak phase ϕ_s and the decay width difference $\Delta\Gamma_s$ in the decay $B^0_s \rightarrow J/\psi\phi$

4.1 Maximum Likelihood Fit

For the determination of the physics parameters we are interested in, an unbinned maximum likelihood fit of the measured physics variables of selected B^0_s candidates is performed. A total of 26 parameters are determined, including eight physics parameters: three parameters of the B^0_s system (CP-violation weak mixing phase ϕ_s, decay width Γ_s and decay width difference $\Delta\Gamma_s$) and five parameters related to the decay amplitudes. The remaining parameters describe the J/ψ mass distribution, the decay time and the angular distribution of the background.

There are three angular momentum states in the decay $B^0_s \rightarrow J/\psi\phi$, combined in three different polarisation states at proper time zero: one longitudinal polarisation $A_0(0)$ and two transverse polarisations, one with the polarisation of the vector mesons parallel to each other $A_\parallel(0)$ and one with the polarisation vectors perpendicular to each other $A_\perp(0)$. In terms of CP-eigenstates the first two states are CP-even whereas the third one is CP-odd. Due to contamination of non-resonant $B^0_s \rightarrow J/\psi K^+K^-$ and $B^0_s \rightarrow J/\psi f_0$ decays, another CP-odd state can be produced, adding a fourth independent S-wave amplitude $A_S(0)$. Due to normalisation $|A_0(0)|^2 + |A_\parallel(0)|^2 + |A_\perp(0)|^2 + |A_S(0)|^2 = 1$ only three of the four amplitudes are free parameters.

Each amplitude A_i comes with an associated strong phase δ_i. Because only differences between the phases can be measured, one phase is arbitrary, i.e. we use the convention $\delta_0 = 0$. Due to the absence of initial state flavour tagging the analysis is not sensitive to $\delta_\perp$. Consequently the two strong phases $\delta_\parallel$ and δ_S will be determined by the fit. Furthermore, without flavour tagging the PDF is invariant under the transformation

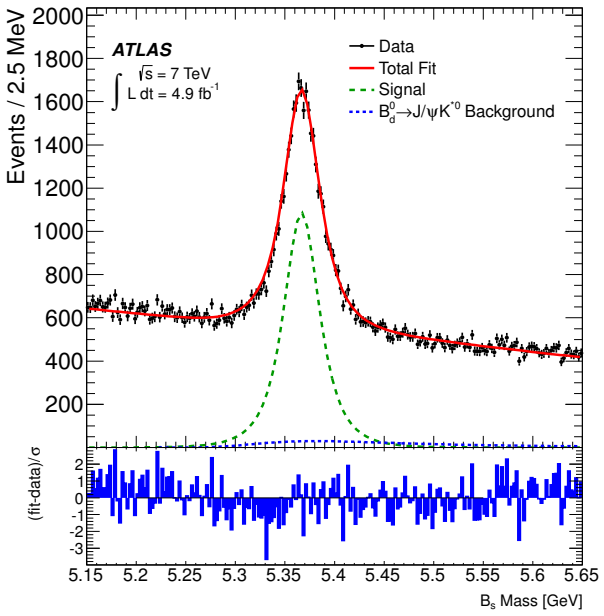

Figure 3: Mass fit projection for the B_s^0. The pull distribution at the bottom shows the difference between the data and fit value normalised to the data uncertainty [5].

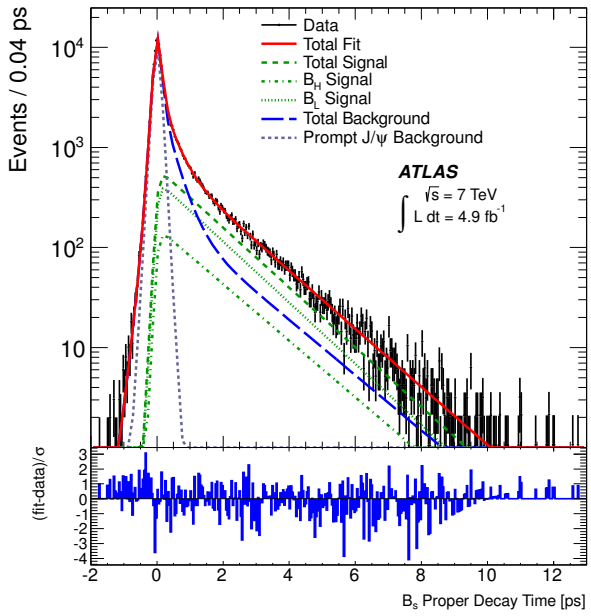

Figure 4: Proper decay time fit projection for the B_s^0. The pull distribution at the bottom shows the difference between the data and fit value normalised to the data uncertainty [5].

$\{\phi_s, \Delta\Gamma_s, \delta_\perp, \delta_\parallel, \delta_S\} \to \{\pi - \phi_s, -\Delta\Gamma_s, \pi - \delta_\perp, -\delta_\parallel, -\delta_S\}$ as well as $\{\phi_s, \Delta\Gamma_s, \delta_\perp, \delta_\parallel, \delta_S\} \to \{-\phi_s, \Delta\Gamma_s, \pi - \delta_\perp, -\delta_\parallel, -\delta_S\}$. Therefore the parameter $\delta_\perp$ is fixed by a Gaussian constraint from LHCb measurements $\delta_\perp = (2.95 \pm 0.39)$ rad [12].

The unbinned maximum likelihood fit uses the information of the reconstructed B_s^0 as the invariant mass, the proper decay time and their uncertainties as well as the transversity angles of the final state particles [14].

4.2 Results

Maximising the likelihood function gives the best fit parameters. Results not consistent with the constraints from LHCb measurements [12, 13] are excluded. The most interesting physics parameters are summarised in Table 2. The strong phase $\delta_\parallel$ is fitted close to π, but due to non-Gaussian pull distributions for this parameter the result of $\delta_\parallel$ is given as the 1σ confidence interval $[3.04, 3.24]$ rad. The phase of the S-wave component is fitted relative to $\delta_\perp$ with the best fit value $\delta_\perp - \delta_S = (0.03 \pm 0.13)$ rad. The amplitude for the S-wave contribution due to non-resonant K^+K^- and f_0 contamination is found to be consistent with zero.

The systematic uncertainties of the parameters are assigned by considering effects that cannot be obtained by the maximum likelihood fit. Systematics of the fit model are determined by pseudo-experiments with varied signal and background mass models, resolution models, background lifetime and background angle models. The largest contribution comes from the variation of the background angle models.

The fit projections for the B_s^0 mass variable and the B_s^0 proper decay time variable are shown in Figure 3 and Figure 4, respectively. In the mass fit projection the peak of 22 700 B_s^0 signal events on top of a large background contamination is clearly visible. The reason for this large background contribution can be seen in the Figure 4: while in measurements by LHCb a lifetime cut is applied on the B_s^0 candidates, in ATLAS this is avoided. The large peak around $t \sim 0$ is mainly due to events with prompt J/ψ's produced directly in pp collisions. The main advantage of not doing a lifetime cut is that the events around $t \sim 0$ allow to better measure the properties of background events, as e.g. the angular distributions, and consequently helps to distinguish between the CP-eigenstates.

In Figure 5 the two parameters most sensitive for new physics beyond the SM are shown as a two-dimensional

Table 2: Fitted values for the physics parameters and their statistical and systematic uncertainties. Table taken from [5].

Parameter	Value	Stat.	Syst.
ϕ_s(rad)	0.22	0.41	0.10
$\Delta\Gamma_s$(ps^{-1})	0.053	0.021	0.010
Γ_s(ps^{-1})	0.677	0.007	0.004
$\lvert A_0(0)\rvert^2$	0.528	0.006	0.009
$\lvert A_\parallel(0)\rvert^2$	0.220	0.008	0.007
$\lvert A_S(0)\rvert^2$	0.02	0.02	0.02

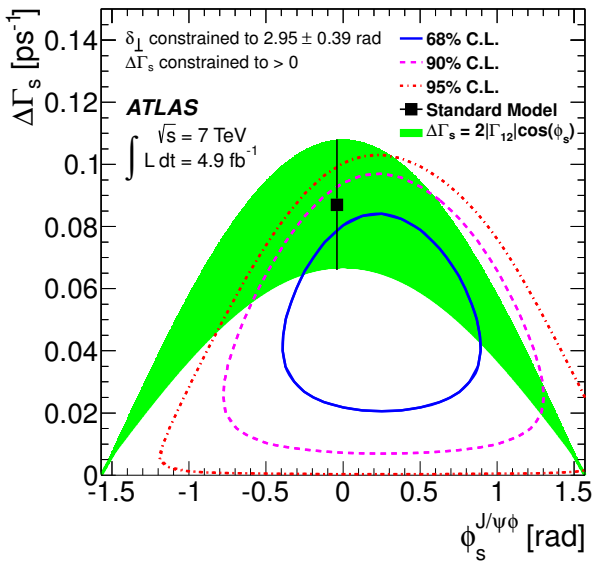

Figure 5: Likelihood contours in the $\phi_s - \Delta\Gamma_s$ plane. Three contours show the 68 %, 90 % and 95 % confidence intervals (statistical errors only). The green band is the theoretical prediction of mixing-induced CP-violation. The PDF contains a fourfold ambiguity. Three minima are excluded by applying the constraints from the LHCb measurements. Figure taken from [5].

likelihood contour plot for 68 %, 90 % and 95 % confidence intervals. By using a profile likelihood method, these contours do not include the systematic uncertainties, but as shown in Table 2 they are small compared to the statistical uncertainties. In previous measurements by LHCb with flavour tagging and consequently sensitive to the measurement of $\delta_\perp$, only solutions with a positive ϕ_s and two $\Delta\Gamma_s$ values symmetric around zero are quoted. Further more, solutions with negative $\Delta\Gamma_s$ are excluded by another LHCb measurement [13]. Since in the ATLAS measurement $\delta_\perp$ is constrained by LHCb measurements, only the solution compatible with these measurements is shown in Figure 5.

5 Summary and Outlook

From 2.4 fb^{-1} of data collected in pp collisions at $\sqrt{s}$ = 7 TeV by the ATLAS experiment in 2011 an upper limit on the branching ratio $\mathcal{B}(B_s^0 \to \mu^+\mu^-) < 2.2(1.9) \times 10^{-8}$ at 95 % (90 %) CL has been set. This result has been used for the first LHC-wide combination of results by ATLAS, CMS and LHCb on $\mathcal{B}(B_s^0 \to \mu^+\mu^-)$ [9]. An update of the ATLAS result with more data is about to be published.

Using 4.9 fb^{-1} of data the decay time and angular distributions of about 22 700 $B_s^0 \to J/\psi(\mu^+\mu^-)\phi(K^+K^-)$ events have been analysed. In absence of initial state flavour tagging and assuming $\delta_\perp = (2.95 \pm 0.39)$ rad we obtain a value for the CP-violation weak mixing phase $\phi_s = 0.22 \pm 0.41\,(\text{stat.}) \pm 0.10\,(\text{syst.})$ rad and $\Delta\Gamma_s = 0.053 \pm 0.021\,(\text{stat.}) \pm 0.10\,(\text{syst.})\,\text{ps}^{-1}$ the decay width difference.

In data with pp collisions at a centre of mass energy of $\sqrt{s}$ = 8 TeV the thresholds on the trigger transverse momentum are increased. As a consequence the proper time resolution is increased at the expense of event rate. In order to increase the precision of the ϕ_s measurement ATLAS plans to distinguish the initial B_s^0 state using flavour tagging.

Acknowledgements

This work was supported by the Austrian Ministry of Science and Research (BM.WF) and the Austrian Science Fund (FWF) project P22982. Copyright CERN for the benefit of the ATLAS collaboration.

References

[1] K. De Bruyn, R. Fleischer et.al., Phys. Rev. Lett. **109** (2012) 041801, [arXiv:1204.1737].
[2] UTFit Collaboartion, Phys. Rev. Lett. **97** (2006) 151803, [hep-ph/0605213].
[3] A. Lenz, U. Nierste, JHEP **0706** (2007) 072, [hep-ph/0612167].
[4] ATLAS Collaboration, Phys. Lett. **B713** (2012) 387, [arXiv:1204.0735].
[5] ATLAS Collaboration, to appear in J. High Energy Phys., [arXiv:1208.0572].
[6] ATLAS Collaboration, JINST **3** (2008) S08003.
[7] T. Junk, Nucl. Inst. Meth. **A434** (1999) 435, [hep-ex/9902006].
[8] A.L. Read, J. Phys. **G28** (2002) 2693.
[9] ATLAS, CMS and LHCb Collaboration, ATLAS-CONF-2012-061 [http://cds.cern.ch/record/1456262], CMS-PAS-BPH-12-009, LHCb-CONF-2012-017.
[10] Particle Data Group, K. Nakamura et. al., J. Phys. **G37** (2010) 075021, [http://pdg.lbl.gov/].
[11] LHCb Collaboration, Phys. Rev. D **85** (2012) 032008, [arxiv:1111.2357].
[12] LHCb Collaboration, Phys. Rev. Lett. **108** (2012) 101803, [arxiv:1112.3183].
[13] LHCb Collaboration, Phys. Rev. Lett. **108** (2012) 241801, [arxiv:1202.4717].
[14] A.S. Dighe, I. Dunietz and R. Fleischer, Eur. Phys. J. **C6** (1999) 647, [hep-ph/9804253].